Available online at www.sciencedirect.com
SCIENCE DIRECT®
Catalysis Today 86 (2003) 31–43
CATALYSIS TODAY
www.elsevier.com/locate/cattod

A model catalyst approach to the effects of the support on Co–Mo hydrodesulfurization catalysts

Yasuaki Okamoto*, Takeshi Kubota

Department of Material Science, Shimane University, Matsue 690-8504, Japan

Received 1 March 2003; received in revised form 15 April 2003; accepted 19 May 2003

Abstract

Co–Mo model sulfide catalysts, in which CoMoS phases are selectively formed, were prepared by means of a CVD technique using $Co(CO)_3NO$ as a precursor of Co. It is shown by means of XPS, FTIR and NO adsorption that CoMoS phases form selectively when the Mo content exceeds monolayer loading. A single exposure of MoS_2/Al_2O_3 to a vapor of $Co(CO)_3NO$ at room temperature fills the edge sites of the MoS_2 particles. It is suggested that the maximum potential HDS activity of MoS_2/Al_2O_3 and Co–Mo/Al_2O_3 catalysts can be predicted by means of $Co(CO)_3NO$ as a "probe" molecule. An attempt was made to determine the fate of $Co(CO)_3NO$ adsorbed on MoS_2/Al_2O_3. The effects of the support on Co–Mo sulfide catalysts in HDS and HYD were investigated by use of CVD-Co/MoS_2/support catalysts. XPS and NO adsorption showed that model catalysts can also be prepared for SiO_2-, TiO_2- and ZrO_2-supported catalysts by means of the CVD technique. The thiophene HDS activity of CVD-Co/MoS_2/Al_2O_3, CVD-Co/MoS_2/TiO_2 and CVD-Co/MoS_2/Al_2O_3 is proportional to the amount of Co species interacting with the edge sites of MoS_2 particles or CoMoS phases. It is concluded that the support does not influence the HDS reactivity of CoMoS phases supported on TiO_2, ZrO_2 and Al_2O_3. In contrast, CoMoS phases on SiO_2 show catalytic features characteristic of CoMoS Type II. With the hydrogenation of butadiene, on the other hand, the Co species on MoS_2/TiO_2, ZrO_2 and SiO_2 have the same activity, while the Co species on MoS_2/Al_2O_3 have a higher activity.

Keywords: Effect of support; Hydrodesulfurization; Co–Mo catalyst; Model catalyst; MoS_2 catalyst; Hydrogenation

1. Introduction

In United States, Europe and Japan, the development of highly active hydrodesulfurization (HDS) catalysts to obtain cleaner fuels is being given top priority. Al_2O_3-supported Co(Ni)–Mo sulfide catalysts have been used extensively for industrial HDS. Numerous studies [1–10] have been conducted of the catalytic synergies between Co(Ni) and Mo, the structure of active sites, HDS reaction mechanism and the effects of the support in order to design and prepare highly active HDS catalysts. Since the proposal of Topsøe and co-workers [1,3,11–15], there has been growing interest in so-called CoMoS or NiMoS phases, in which Co(Ni) decorates the edge sites of highly dispersed MoS_2 particles. These phases may be catalytically active sites in Co(Ni)–Mo sulfide catalysts and many catalytic and spectroscopic aspects of Co(Ni)–Mo sulfide catalysts have been interpreted in terms of the phases. Candia et al. [15] differentiated between two CoMoS phases, Type I and Type II, depending on their intrinsic HDS activity. CoMoS Type II, which was formed by high-temperature sulfidation at 873–1275 K, was about twice as active as Type I formed by sulfidation at 675 K. TEM and XPS [15–17] showed that changes in

* Corresponding author. Fax: +81-852-32-6466.
E-mail address: yokamoto@riko.shimane-u.ac.jp (Y. Okamoto).

0920-5861/$ – see front matter © 2003 Elsevier B.V. All rights reserved.
doi:10.1016/S0920-5861(03)00402-4

the stacking number of MoS_2 slabs lead to the different types of CoMoS phases. Accordingly, the formation of highly dispersed CoMoS Type II may result in highly active Co–Mo sulfide catalysts. Hence, the control of the morphology, size and stacking number, of supported MoS_2 particles is of paramount importance for the design of highly active HDS catalysts. The effects of the support and additives such as fluorine, phosphorous and boron modify the interaction between the Mo oxides and the support, thus resulting in a change in the morphology of MoS_2 in sulfided catalysts [18,19]. Detailed studies of the effects of the support and additives on HDS performance are promising for the development of catalysts for ultra-clean fuels. However, because practical Co(Ni)–Mo sulfide catalysts, supported on refractory oxides, are inherently heterogeneous [1], it is difficult to understand the active sites and the effects of the support and additives.

The catalytic activities of Mo and Co(Ni)–Mo sulfide catalysts in HDS are greatly affected by the support [10,18,20]. Selective preparation of CoMoS phases would provide insight into the nature of these effects. By means of in situ ^{57}Co Mössbauer emission spectroscopy, van Veen et al. [21,22] demonstrated that CoMoS Type II is selectively prepared by adding nitrilotriacetic acid (NTA) to the impregnation solutions. Prins and co-workers [19,23,24] and van Veen et al. [25] reported that NTA is also effective for the selective preparation of NiMoS phases on SiO_2, Al_2O_3 and active carbon. van Veen et al. [21] showed that the intrinsic HDS activity of CoMoS Type II phases supported on activated carbon is twice as high as the intrinsic activity of CoMoS Type II supported on Al_2O_3 or SiO_2. Bouwens et al. [17] confirmed similar activity for CoMoS Type II. Based on Co and Mo K-edge EXAFS, they reported the formation of two types of the CoMoS phase, the Co species of which have different structures.

Another method, which would lead to the selective formation of CoMoS phases, is to use cobalt carbonyls as a precursor. Maugé et al. [26,27] introduced $Co(CO)_3NO$ to sulfided Mo/Al_2O_3 and thermally decomposed it prior to HDS. They found that the ex-carbonyl catalysts are twice as active as a conventional $Co–Mo/Al_2O_3$ catalyst. The HDS activity of the ex-carbonyl catalysts increased linearly with the amount of Co introduced, suggesting a selective formation of CoMoS phases. Angulo et al. [28] prepared $Ni–Mo/Al_2O_3$ by using $Ni(CO)_4$, demonstrating a higher degree of promotion than conventional catalysts. Halbert et al. [29] used $Co_2(CO)_8$ as a precursor for the modification of unsupported MoS_2 and sulfided Mo/Al_2O_3. It was found that the HDS activity is rather high compared to the activities of corresponding impregnation catalysts. In a similar study, Okamoto et al. [30] modified Al_2O_3-supported Mo sulfide catalysts prepared from $Mo(CO)_6$ with a vapor of $Co_2(CO)_8$. They claimed the preferential formation of a CoMoS phase or Co–Mo sulfide clusters on the Co–Mo sulfide catalysts. These studies, however, did not provide direct evidence of the exclusive formation of CoMoS phases. By means of EXAFS and XPS, our studies [31–33] have shown that Co–Mo sulfide clusters form in zeolite cages when the carbonyl technique is applied. This review paper discusses our recent studies [34,35] of the preparation of Co–Mo model sulfide catalysts, in which Co species, constituting CoMoS phases, are exclusively formed: the use of $Co(CO)_3NO$ as a precursor and the described method of preparation revealed the effects of the support on the performance of Co–Mo sulfide catalysts.

Recently, model catalysts including supported metal sulfides have received attention for better characterizations of these catalyst systems [36]. In these model catalysts, metals, metal oxides or their precursors are supported on a flat surface of thin oxide films on a (semi) conducting material such as silicon by means of a vapor deposition technique or a spin-coating technique. Crystalline surfaces of metal oxides, such as Al_2O_3 and SiO_2, and of metals are also used as model supports.

de Jong et al. [37] studied a model catalyst $Mo/SiO_2/Si(1\,0\,0)$ by means of surface science techniques including XPS, AFM, RBS and SIMS. They revealed the precise sulfidation behavior of Mo oxides supported on the SiO_2 film by means of XPS without broadening due to differential chargings inherent to practical catalysts. Kishan et al. [38,39] used a $SiO_2/Si(1\,0\,0)$ model support for the preparation of Ni–W and Co–W sulfide catalysts to study the effects of chelating agents on the sulfidation behavior of Ni, Co and W. Coulier et al. [40] studied Co–W and $Ni–W/Al_2O_3/Si$ wafer model catalysts to show the effect of the support and a chelating agent. Narrow XPS lines enabled them to reach unambiguous conclusions

that redispersion of preformed bulk Ni sulfides to the edge of WS_2 slabs leads to the formation of NiWS phases, while bulk Co sulfides do not redisperse to form the active phases. Sakashita and Yoneda [41] prepared Mo sulfide catalysts supported on the (1 0 0) and (1 1 1) planes of a γ-Al_2O_3 single crystal. Their HRTEM observations of the flat model catalysts clearly indicated the formation of edge-bonded MoS_2 clusters on the (1 0 0) surface. On the other hand, basal bonded MoS_2 clusters grew on the (1 1 1) surface. It was suggested that the arrangements of Al or O atoms in γ-Al_2O_3 and Mo atoms in MoS_2 determine the orientation of MoS_2 clusters on the Al_2O_3 surfaces.

Recently, by means of STM, Helveg et al. [42] succeeded to observe the atomic scale structure of single-layer MoS_2 triangle clusters fabricated on Au(1 1 1). They concluded that S atoms at the edges are out of registry with the S atoms in the hexagonal lattice of the basal plane. In conjunction with DFT calculations [43], it was suggested that the edges of the clusters are composed of reconstructed Mo edges. In the presence of Co, however, hexagonally truncated MoS_2 nanoclusters are formed, suggesting the preferential location of Co atoms at the S-edges of MoS_2 [44]. The sulfur vacancies were observed by means of STM to form on the edges of MoS_2 clusters by contact with atomic hydrogen [43–45]. The thiophene adsorption and subsequent reaction were also detected in atomic scale on H_2-adsorbed MoS_2 nanoclusters on Au(1 1 1) by means of STM [45]. The model catalyst approaches are thus promising for better characterization and, accordingly, better understandings of hydrotreating catalysts.

The “model” catalysts in our study are much more practical than the model catalysts mentioned above, but will, nevertheless, provide important insight into the nature of HDS catalysts.

1.1. Preparation of supported Co–Mo model sulfide catalysts

Al_2O_3-supported Mo oxide catalysts containing various amounts of Mo were prepared by means of impregnation with ammonium paramolybdate. The resulting Mo/Al_2O_3 was sulfided at 673 K for 1.5 h to form MoS_2/Al_2O_3, followed by evacuation at 673 K. MoS_2/Al_2O_3 was then exposed to a vapor of $Co(CO)_3NO$ at room temperature (CVD technique). After evacuation at room temperature, $Co(CO)_3NO/MoS_2/Al_2O_3$ was sulfided again at 673 K to prepare a $Co–Mo/Al_2O_3$ catalyst. The resulting catalyst is designated CVD-$Co/MoS_2/Al_2O_3$.

Fig. 1 shows the catalytic activity of MoS_2/Al_2O_3 in the HDS of thiophene as a function of Mo content. The maximum activity of MoS_2/Al_2O_3 was attained with around 10–15 wt.% Mo, in agreement with others [1,2,46]. As shown in Fig. 1, the addition of Co by means of the CVD technique greatly enhanced the HDS activity. The activity of CVD-$Co/MoS_2/Al_2O_3$ was hardly dependent on the Mo content between 6 and 22 wt.%. Fig. 2 gives the amount of Co incorporated into MoS_2/Al_2O_3 as a function of Mo content. A considerable amount of Co was deposited, even when the Al_2O_3 support was exposed to a vapor of $Co(CO)_3NO$ (CVD-Co/Al_2O_3). The amount of Co increased as the Mo content increased to 7 wt.%. After reaching a maximum at 7 wt.% Mo, the Co content decreased as the Mo loading increased and leveled off at a Mo content greater than 14 wt.%. The dispersion of the MoS_2 particles in MoS_2/Al_2O_3 was evaluated by NO adsorption (pulse technique). The amounts of NO adsorption are presented in Table 1. The NO/Mo ratio decreased as the Mo content increased, in agreement with the results obtained by others [1,47,48].

In order to examine the location of Co deposited by the CVD technique, the Co/Mo ratio is plotted against the NO/Mo ratio (Fig. 3). When the Mo loading was larger than 9 wt.%, the Co/Mo ratio of the MoS_2/Al_2O_3 catalysts was proportional to the NO/Mo ratio (including the results in Fig. 11, vide infra). It has been established [1] that NO molecules adsorb on the edge sites of MoS_2 particles rather than on the basal plane. Hence, the plot in Fig. 3 strongly suggests that Co is located on the edge sites of MoS_2 particles at $\geqq$9 wt.% Mo. According to the literature [48–51], a monolayer dispersion of Mo oxides is attained around 8.5 wt.% Mo (3 Mo atoms nm^{-2}) in the present series of Mo/Al_2O_3 (Al_2O_3, 177 $m^2\,g^{-1}$). The Co 2p XPS spectra of CVD-Co/Al_2O_3 and CVD-$Co/MoS_2/Al_2O_3$ (8.7 wt.% Mo) are presented in Fig. 4. The Co $2p_{3/2}$ binding energy for CVD-Co/Al_2O_3 was close to that of Co_9S_8, indicating that Co sulfide clusters formed as expected. However, in the presence of MoS_2 particles, the Co $2p_{3/2}$ binding energy increased by 0.9 eV, clearly demonstrating that Co species chemically interact with the edge sites of MoS_2 particles. In line

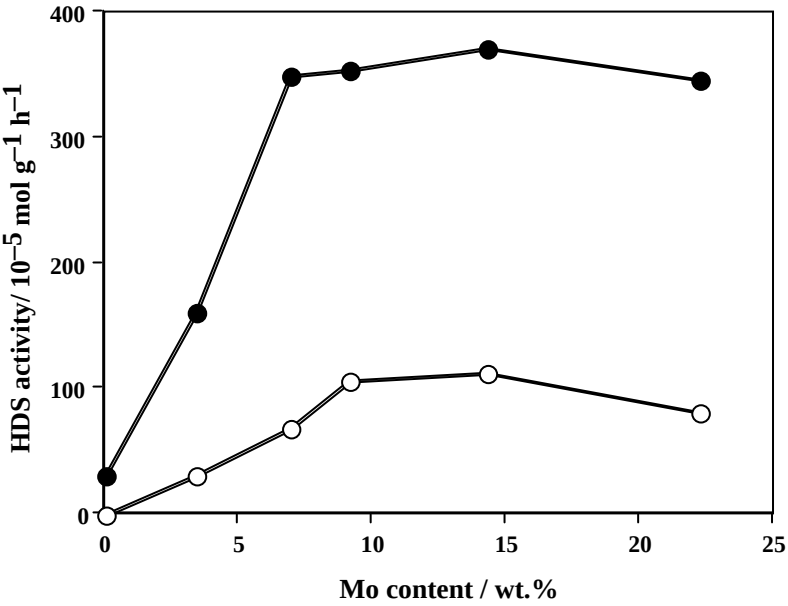

Fig. 1. HDS activities of MoS_2/Al_2O_3 (○) and CVD-Co/MoS_2/Al_2O_3 (●) as a function of Mo content [34].

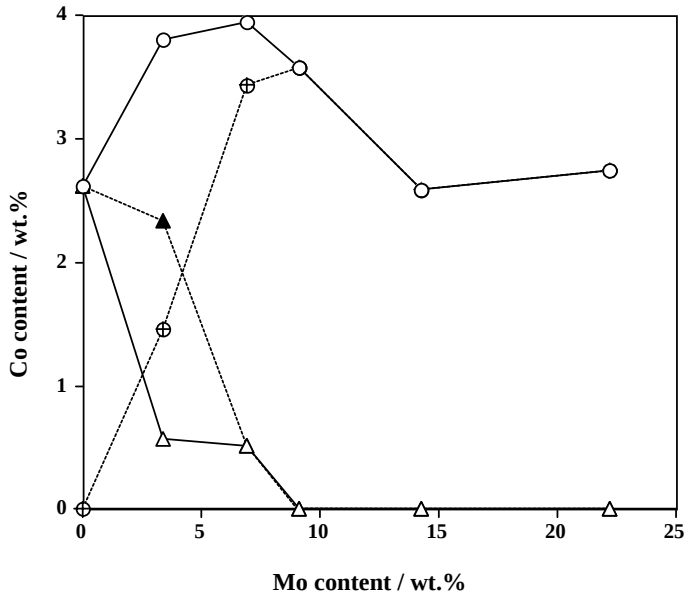

Fig. 2. Amount of Co species in CVD-Co/MoS_2/Al_2O_3 as a function of Mo content: (○) the total amount of Co accommodated by the CVD technique; (△) the amount of Co sulfide clusters produced by the interaction with basic sites of Al_2O_3; (▲) the total amount of separate Co sulfide clusters; and (⊕) the amount of Co species, which form CoMoS phases, as estimated from the HDS activity and Co content [34].

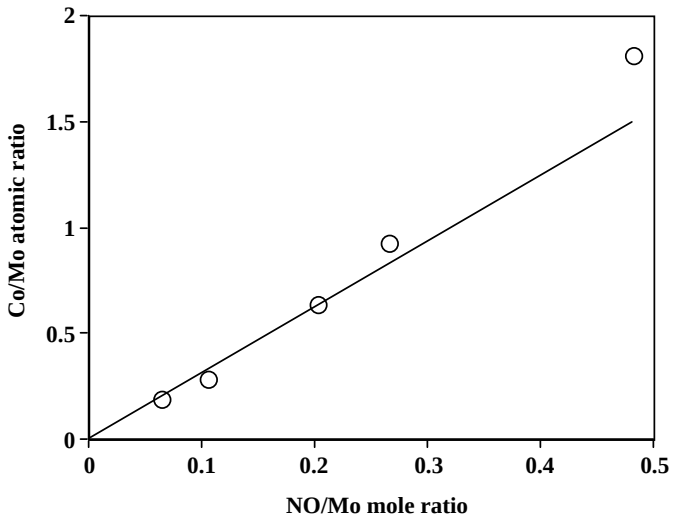

Fig. 3. Correlation between the NO/Mo mole ratio for MoS_2/Al_2O_3 and the Co/Mo atomic ratio for CVD-Co/MoS_2/Al_2O_3 [34].

with the present XPS results, Alstrup et al. [52] reported that the Co $2p_{3/2}$ binding energy was 0.6 eV higher for CoMoS than for Co_9S_8. The increase in the Co content (Fig. 2) in the presence of Mo also suggests interactions of Co with Mo sulfide phases, as reported previously [30]. Furthermore, the FWHM of the Co 2p spectrum of CVD-Co/MoS_2/Al_2O_3 is considerably narrower than that of CVD-Co/Al_2O_3. In agreement with the conclusion from the chemical shift, this indicates that the spectral broadening due to differential charging for CVD-Co/Al_2O_3, caused by direct contact of Co sulfide clusters with the Al_2O_3 surface, is removed by the preferential interaction of Co atoms with the edge of the MoS_2 particles. The preferential interaction of $Co(CO)_3NO$ with the Mo sulfide phase was also suggested by Maugé et al. [27] by means of the FTIR of CO adsorption.

Table 1
Amount of NO adsorption of MoS_2/Al_2O_3[a] and the Co content of CVD-Co/MoS_2/Al_2O_3

Mo content (wt.%)	NO/Mo (mol mol^{-1})	Co content (wt.%)	Co/Mo atomic ratio
0	–	2.61	–
3.4	0.480	3.80	1.81
6.9	0.265	3.95	0.93
9.1	0.202	3.58	0.64
14.3	0.104	2.59	0.29
22.2	0.063	2.74	0.20

[a] Al_2O_3, JRC-ALO-4.

For MoS_2/Al_2O_3 catalysts with a Mo content less than a monolayer loading, the Co/Mo ratio was slightly higher than that expected from the linear line in Fig. 3. This may indicate the presence of excess Co

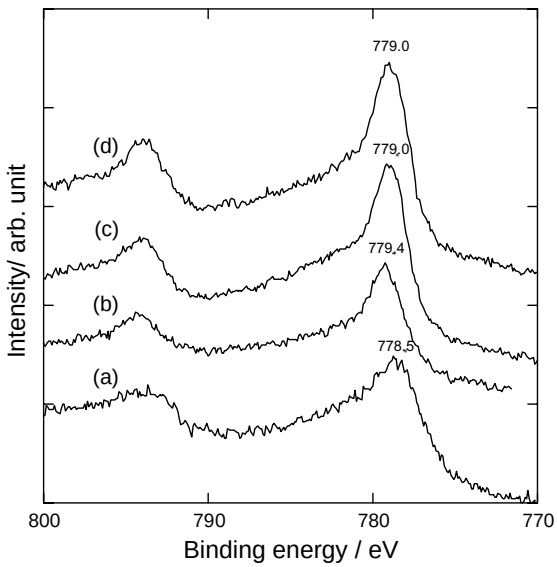

Fig. 4. Co 2p XPS spectra for (a) CVD-Co/Al_2O_3, (b) CVD-Co/MoS_2/Al_2O_3, (c) CVD-Co/MoS_2/Al_2O_3 exposed again to a vapor of $Co(CO)_3NO$, followed by sulfidation and (d) Co–Mo/Al_2O_3 prepared by an impregnation. The Co $2p_{3/2}$ binding energies (eV) are shown in the figure [35].

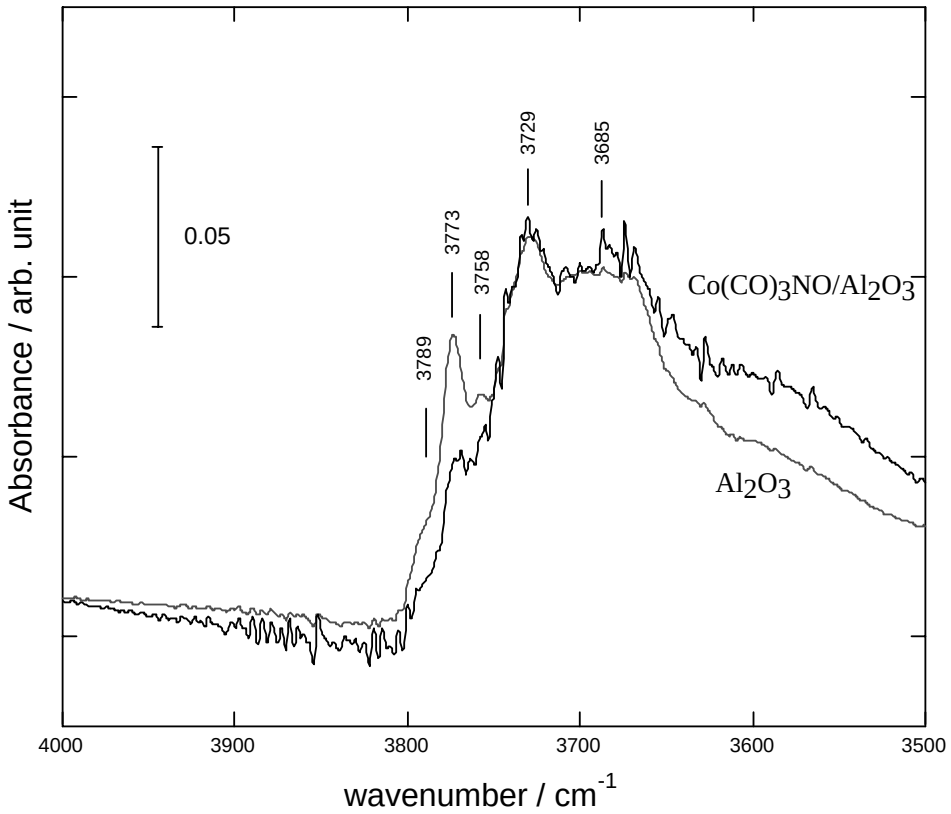

Fig. 5. FTIR spectra of the hydroxyl groups of Al_2O_3. Solid line: after evacuation at 773 K and dotted line: after adsorption of $Co(CO)_3NO$ [35].

species compared to the amount of Co species which interact with MoS_2 phases. It is considered that these excess Co species interact with the bare Al_2O_3 surface. Accordingly, it is concluded that, when the Mo content of MoS_2/Al_2O_3 exceeds a monolayer loading, CoMoS phases are preferentially formed by using $Co(CO)_3NO$ as a precursor [34]. These results are explained by a competitive interactions of Mo species and $Co(CO)_3NO$ with the surface basic hydroxyl groups of Al_2O_3. The FTIR spectra (Fig. 5) indicate a preferential interaction of $Co(CO)_3NO$ with the most basic OH^- groups at 3787 and 3773 cm^{-1}. When the Mo content is high enough to consume all the basic hydroxyl groups on Al_2O_3 (3 Mo atoms nm^{-2} or monolayer composition [51]), $Co(CO)_3NO$ molecules preferentially interact with the MoS_2 edge sites (coordinatively unsaturated sulfur atoms) [27,34]. The $Co(CO)_3NO$ molecules are transformed into CoMoS phases on the second sulfidation at 673 K. Furthermore, it was shown [34] that when Mo/Al_2O_3 is not calcined, an excess amount of Co is anchored on the bare Al_2O_3 surface even for a monolayer catalyst because part of basic hydroxyl groups remains intact due to incomplete reactions with Mo oxide phases. The amount of $Co(CO)_3NO$ fixed on the Al_2O_3 surface was 2.61 wt.% Co or 1.5 Co atoms nm^{-2} and was very close to the maximum amount of Mo oxide species in tetrahedral configurations, Mo_{tet}, on Al_2O_3 (1.7 Mo atoms nm^{-2} [51]), which is formed by the consumption of the basic hydroxyl groups. The $Co(CO)_3NO$ molecules adsorbed on Mo oxysulfide species formed from Mo_{tet} oxide species are transformed to Co sulfide clusters [34].

When the catalyst was exposed again to a vapor of $Co(CO)_3NO$ and resulfided, the HDS activity of CVD-$Co/MoS_2/Al_2O_3$ hardly changed (Table 2).

Table 2
Amount of anchored Co and the catalytic activity for the HDS of thiophene as a function of the number of the CVD cycle

Number of CVD cycle	Co content (wt.%)	HDS activity[a]
0	0	83
1	2.61	314
2	4.49	304

[a] 10^{-5} mol g^{-1} h^{-1} at 623 K.

The Co content increased by a factor of 1.7 after the second addition of $Co(CO)_3NO$. It is concluded that applying CVD once (5 min at room temperature) fills the edge sites of MoS_2 particles with Co atoms, constituting CoMoS phases, and that $Co(CO)_3NO$ molecules adsorbed on the edge sites of Co–MoS_2 particles are transformed into separate Co sulfide clusters. Consistent with the results in Table 2, the Co $2p_{3/2}$ binding energy of CVD-Co/MoS_2/Al_2O_3 was reduced by 0.4 eV after the second addition of Co (Fig. 4).

Fig. 6 presents the FTIR spectra of NO adsorption on CVD-Co/MoS_2/Al_2O_3, CVD-Co/Al_2O_3, MoS_2/Al_2O_3 and a conventional Co–Mo/Al_2O_3 impregnation catalyst. With the latter catalyst, there may be two sets of doublets due to dinitrosyl species on Mo (1690 and 1780 cm^{-1}) and Co (1790 and 1850 cm^{-1}), as many groups have reported [1,53,54]. On the contrary, CVD-Co/MoS_2/Al_2O_3 showed essentially a single doublet (1810 and 1855 cm^{-1}) ascribed to NO adsorbed on Co sites. This is in accord with the activity reported in Table 2. Furthermore, all the edge sites of MoS_2 particles that are accessible to NO adsorption are covered by Co atoms constituting CoMoS phases.

Fig. 7 shows what happened to the $Co(CO)_3NO$ molecules adsorbed on sulfided MoS_2/Al_2O_3 and Co–Mo/Al_2O_3 [34]. Table 2 and Fig. 7 indicate that the maximum potential HDS activity of the MoS_2/Al_2O_3 and Co–Mo/Al_2O_3 catalysts under study can be predicted by using $Co(CO)_3NO$ as a "probe" molecule.

1.2. Effects of the support on Co–Mo sulfide catalysts

We examined the effect of the support on Co–Mo sulfide catalysts by preparing the catalysts in the same

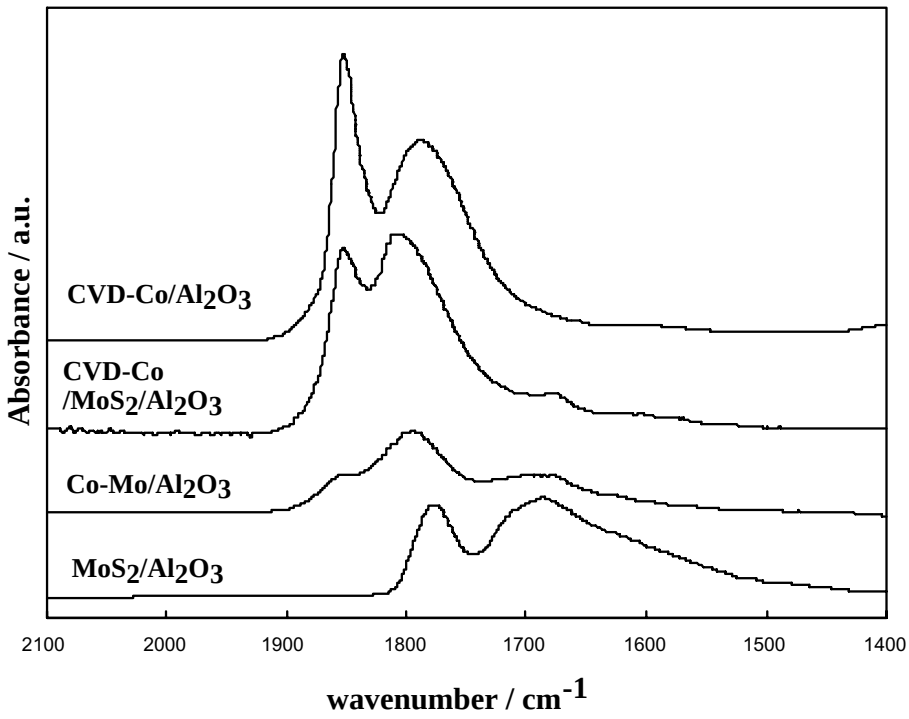

Fig. 6. FTIR spectra of NO adsorption on CVD-Co/MoS_2/Al_2O_3, CVD-Co/Al_2O_3, MoS_2/Al_2O_3 and a 2 wt.% Co–Mo/Al_2O_3 impregnation catalyst.

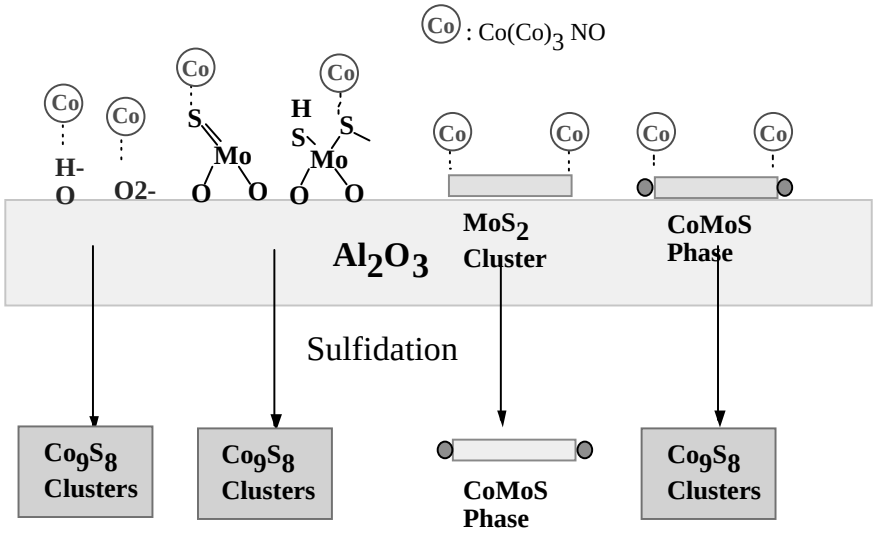

Fig. 7. Schematic model showing the fate of adsorbed $Co(CO)_3NO$ molecules on the sulfidation.

way as the model catalysts. The supports employed were SiO_2, ZrO_2, TiO_2 and Al_2O_3. Table 3 gives the surface area of the support and the Mo content. The Mo content of the catalyst was fixed approximately at its monolayer loading. The dispersion of MoS_2 particles was measured by means of NO adsorption. Table 3 also presents the NO/Mo mole ratio.

Fig. 8 shows a comparison of the turnover frequency (TOF) of the thiophene HDS for the Mo sulfide catalyst; TOF was calculated on the basis of the adsorption capacity of NO. The TOF value for MoS_2/SiO_2 was 1.6 times higher than the values for MoS_2/TiO_2 and MoS_2/ZrO_2. The TOF of the latter catalysts was twice as high the TOF of MoS_2/Al_2O_3 in agreement with others [10,20,46,55,56]. According to Wang et al. [57], the rate constant k_{ex} of the sulfur exchange reaction between dibenzothiophene (DBT) and Mo sulfide particles during the HDS reaction of

Table 3
Mo catalysts used, the dispersion of Mo sulfides and the amount of Co incorporated after sulfidation at 673 K

Support	Surface area ($m^2\,g^{-1}$)	Mo loading (wt.%)	NO/Mo (mol mol^{-1})	Co (wt.%)	Co/Mo atomic ratio
Al_2O_3	177	–		2.61	–
		8.66	0.161	2.86	0.538
				2.72[a]	0.511[a]
			0.275	2.65[b]	0.498[b]
		13.3	0.097	2.36	0.289
SiO_2	347	–		0.15	–
		6.67	0.074	0.98	0.239
		13.3	0.019	0.96	0.117
TiO_2	50	–		2.26	–
		4.0	0.210	1.92	0.781
ZrO_2	25	–		1.65	–
		2.0	0.209	1.07	0.871

[a] $Co(CO)_3NO$ was thermally decomposed at 673 K for 1 h in vacuo before the sulfidation.
[b] H_2-treated at 673 K for 30 min prior to the adsorption of $Co(CO)_3NO$.

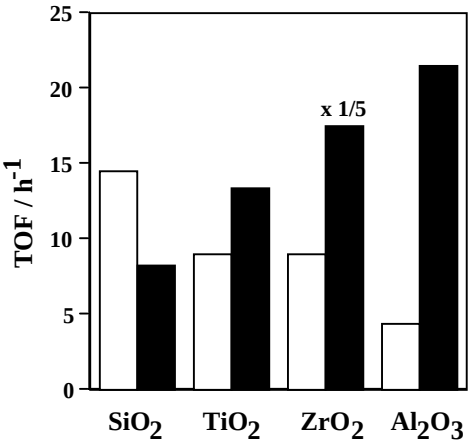

Fig. 8. TOF of the thiophene HDS at 623 K (open bar) and butadiene HYD at 473 K (closed bar) calculated on the basis of the NO adsorption for the supported Mo sulfide catalysts: MoS_2/A_2O_3 (8.7 wt.% Mo), MoS_2/ZrO_2 (2.0 wt.% Mo), MoS_2/TiO_2 (4.0 wt.% Mo) and MoS_2/SiO_2 (6.7 wt.% Mo) [35].

DBT depends on the support and k_{ex} of MoS_2/TiO_2 was larger than that of MoS_2/Al_2O_3. They suggested a promotional effect of Mo–S–Ti bonding. In agreement with their observations, the rate constant k_{Se} of the S–Se exchange reaction during the hydrode-selenium reaction of selenophene over MoS_2/TiO_2 was almost twice that over MoS_2/Al_2O_3 [58,59]. On the other hand, the k_{Se} of MoS_2/SiO_2 differed only slightly to that of MoS_2/Al_2O_3. The rate of the sulfur exchange reaction does not seem to be the rate-determining step in the HDS of thiophene (Fig. 8). The TOF in Fig. 9 probably reflects the interactions between the support and the MoS_2 particles.

Both HDS and hydrogenation (HYD) activity of supported MoS_2 catalysts are very important. The TOF values of the HYD reaction of butadiene over the supported MoS_2 catalysts are compared (Fig. 8). MoS_2/ZrO_2 showed an extraordinarily high TOF of HYD compared with the other catalysts, suggesting the formation of specific active sites on the edges of MoS_2 or on the interface between the MoS_2 particles and the ZrO_2 surface. With the exception of MoS_2/ZrO_2, the TOF of HYD increased as follows: $SiO_2 < TiO_2 < Al_2O_3$. Based on the TEM results in Fig. 9, the average stacking number were 2.9 for MoS_2/SiO_2 and 1.5 for MoS_2/Al_2O_3. The HYD/HDS selectivity [in Fig. 8] seems to be consistent with the rim-edge model proposed by Daage and Chianelli [60]. Effects of the interaction (electronic or geometric)

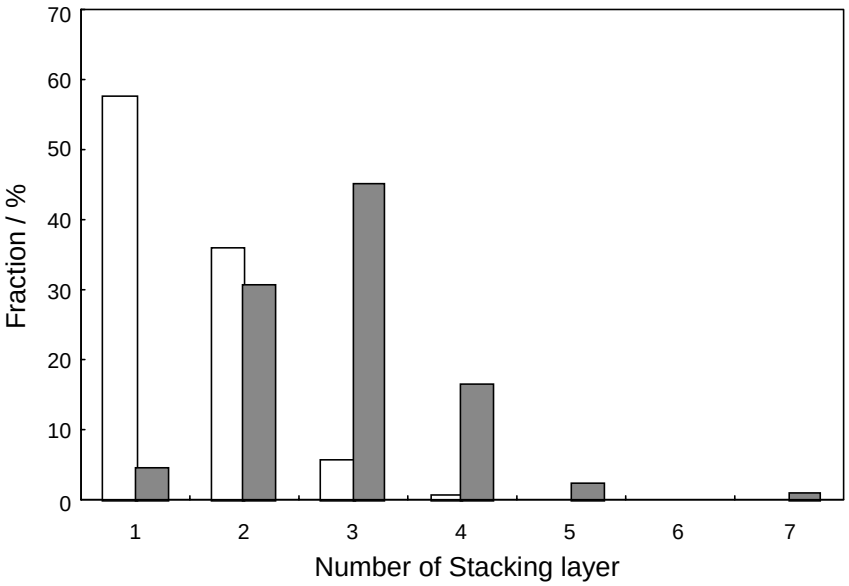

Fig. 9. Distribution of the number of stacking of MoS_2 slabs for MoS_2/Al_2O_3 (9.1 wt.% Mo) and MoS_2/SiO_2 (6.7 wt.% Mo). White bar: MoS_2/Al_2O_3 and black bar: MoS_2/SiO_2.

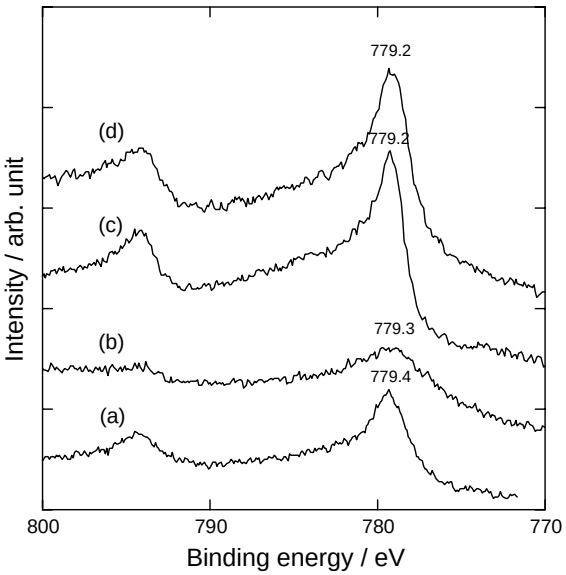

Fig. 10. Co 2p XPS spectra for (a) CVD-Co/MoS_2/Al_2O_3, (b) CVD-Co/MoS_2/SiO_2, (c) CVD-Co/MoS_2/TiO_2 and (d) CVD-Co/MoS_2/ZrO_2. The Co $2p_{3/2}$ binding energies (eV) are shown in the figure [35].

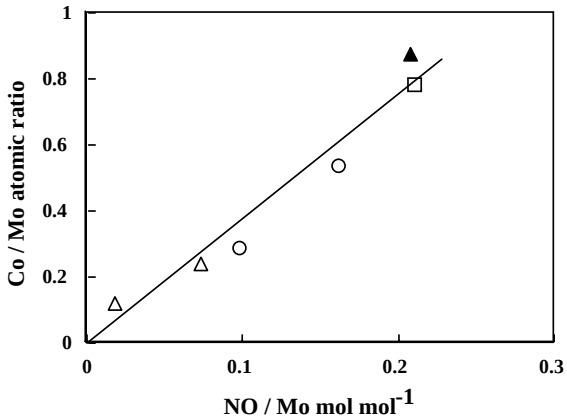

Fig. 11. Correlation between the Co/Mo atomic ratio and the NO/Mo ratio for supported CVD-Co/MoS_2 catalysts: (○) Al_2O_3; (△) SiO_2; (▲) ZrO_2; and (□) TiO_2 [35].

between MoS_2 particles and the support cannot be excluded.

The supported MoS_2 catalysts were exposed to a vapor of $Co(CO)_3NO$ to prepare CVD-Co/MoS_2/support. Table 3 gives the Co content anchored by the CVD procedure and Fig. 10 shows the Co 2p XPS spectra for CVD-Co/MoS_2/support. The Co $2p_{3/2}$ binding energies were 779.3 ± 0.1 eV regardless of the support. Furthermore, the difference in the binding energy of Co $2p_{3/2}$ and S 2p levels was 617.1 ± 0.1 eV, which is characteristic of a Co sulfide species interacting with MoS_2 [52]. These results clearly demonstrate that the Co atoms, introduced by means of the CVD technique, interact with MoS_2 particles on the support.

Fig. 11 shows the Co/Mo ratio of CVD-Co/MoS_2/support as a function of the NO/Mo ratio of the MoS_2/support samples. The Co/Mo ratio is proportional to the NO/Mo ratio, substantiating our findings that Co sulfide species are located on the edge sites of MoS_2 particles. As discussed above, the XPS results showed that the Co species interact with MoS_2 particles. In consequence, we conclude that the Co sulfide species prepared in this way is characteristic of the CoMoS phase proposed by Topsøe et al. [1,3,4] and that the CoMoS phase is preferentially formed when the CVD technique is applied, irrespective of the support. It is concluded that a Co–Mo model catalyst can be prepared, when the Mo content corresponds to or exceeds a monolayer loading in MoS_2/support.

Fig. 12 shows the catalytic activity of CVD-Co/MoS_2/support in the HDS of thiophene as a function of Co loading. A good proportional correlation was obtained for Al_2O_3-, TiO_2- and ZrO_2-supported Co–Mo model catalysts, regardless of the support and the pretreatment (pre-reduced before exposure to $Co(CO)_3NO$ or thermally decomposed after exposure, see Table 3). Since the straight line in Fig. 12 passes through the origin, the activity is ascribed to the Co species interacting with MoS_2 or the CoMoS phase and that there are very few unpromoted Mo sites, if any, after the single adsorption of $Co(CO)_3NO$ in agreement with the FTIR of NO adsorption of CVD-Co/MoS_2/Al_2O_3 (Fig. 6). The TOF of the CoMoS phase (the slope of the line) is identical to that of the Al_2O_3-, TiO_2- and ZrO_2-supported catalysts. We conclude, therefore, that the support has no significant effects on these catalyst systems. The HDS activity of Co–Mo/Al_2O_3, prepared by an impregnation, was somewhat lower than that of CVD-Co/MoS_2/Al_2O_3 with similar Co and Mo loadings (Fig. 12). This is obviously due to the formation of less active Co species

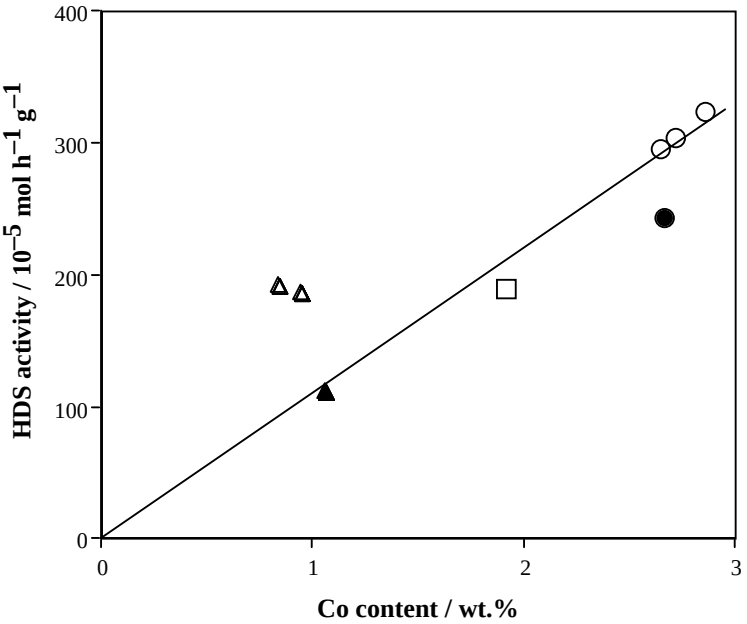

Fig. 12. Correlation between the thiophene HDS activity and the Co loading for supported CVD-Co/MoS_2 catalysts: (○) CVD-Co/MoS_2/Al_2O_3 (8.7); (□) CVD-Co/MoS_2/TiO_2; (▲) CVD-Co/MoS_2/ZrO_2; (△) CVD-Co/MoS_2/SiO_2; and (●) Co–Mo/Al_2O_3 impregnation catalyst [35].

such as Co_9S_8 clusters and Co^{2+} in the Al_2O_3 sublayer in addition to the CoMoS phases, in line with the Co 2p XPS spectrum in Fig. 4.

Fig. 12 shows that the specific activity of the Co species supported on SiO_2 is 1.7 times higher than the activity on the other supports. Taking into account the difference in activity between CoMoS Type I and Type II [15], CoMoS Type I probably forms on the Al_2O_3, TiO_2 or ZrO_2 supports under the present sulfidation conditions (673 K, atmospheric H_2S/H_2), while CoMoS Type II is produced mainly on SiO_2 by the decoration of MoS_2 particles with Co using $Co(CO)_3NO$. It has been claimed [15–17] that CoMoS Type II is present as a multi-layer structure of MoS_2 particles, whereas CoMoS Type I exists as a single slab structure. Our TEM results support this finding and indicate that MoS_2/SiO_2 has a well developed MoS_2 multi-layer structure, whereas MoS_2/Al_2O_3 has a single slab MoS_2 structure (Fig. 9). Based on the model catalysts, we conclude that CoMoS Type I, supported on Al_2O_3, TiO_2 or ZrO_2, has the same TOF of the HDS of thiophene and that CoMoS Type II forms on MoS_2/SiO_2. The number of Co atoms constituting the CoMoS phases was evaluated by means of ^{57}Co Mössbauer emission spectroscopy for conventional Co–Mo catalysts [11–15]. The amount of the CoMoS phases can be determined simply by analyzing the Co content in the Co–Mo model catalysts, if the procedure for preparing the model catalyst is applied.

Fig. 13 presents the catalytic activity of CVD-Co/MoS_2/support for the HYD of butadiene as a function of Co content. The effect of the support was different to that for HDS. The TOF of the HYD on CoMoS phases is identical for SiO_2-, TiO_2- and ZrO_2-supported catalysts, showing that these supports have almost no effect on the reaction, in contrast to the strong effect of the support on the MoS_2/support catalysts (Fig. 8). However, CVD-Co/MoS_2/Al_2O_3 led to a TOF of HYD that was twice as high as that of the other catalysts; but we do not know why. It may be due to different active sites for HDS and HYD and/or different dependence on the electronic state of the CoMoS phases. The results presented in Fig. 13 will be used for designing catalysts for the HDS of FCC gasoline.

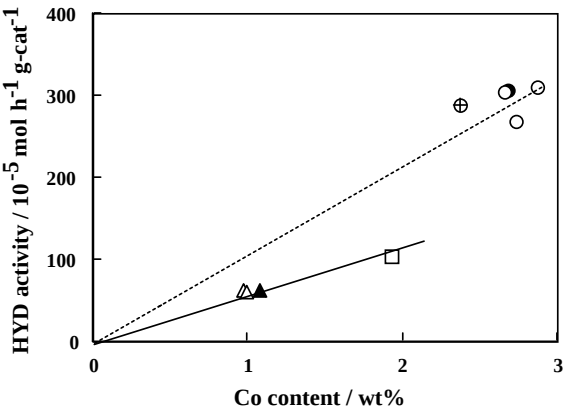

Fig. 13. Correlation between the butadiene HYD activity and the Co loading for supported CVD-Co/MoS_2 catalysts: (○) CVD-Co/MoS_2/Al_2O_3 (8.7); (⊕) CVD-Co/MoS_2/Al_2O_3 (13.3); (□) CVD-Co/MoS_2/TiO_2; (▲) CVD-Co/MoS_2/ZrO_2; (△) CVD-Co/MoS_2/SiO_2; and (●) Co–Mo/Al_2O_3 impregnation catalyst [35].

2. Concluding remarks

CVD-Co/MoS_2/Al_2O_3 model sulfide catalysts, in which CoMoS phases were selectively formed, were prepared by means of a CVD technique using $Co(CO)_3NO$ as the precursor of Co. XPS, FTIR and NO adsorption showed that CoMoS phases are formed selectively when the Mo content exceeds the monolayer loading. A single exposure of MoS_2/Al_2O_3 to a vapor of $Co(CO)_3NO$ at room temperature fills the edge sites of the MoS_2 particles. It is suggested that the maximum potential HDS activity of the MoS_2/Al_2O_3 and Co–Mo/Al_2O_3 catalysts under study can be predicted by using $Co(CO)_3NO$ as a "probe" molecule. The fate of $Co(CO)_3NO$ adsorbed on MoS_2/Al_2O_3 was proposed.

The effects of the support on Co–Mo sulfide catalysts in HDS and HYD were investigated with CVD-Co/MoS_2/support model catalysts. XPS and NO adsorption showed that Co–Mo model catalysts are prepared for SiO_2-, TiO_2-, ZrO_2- and Al_2O_3-supported catalysts by means of the CVD technique. The HDS activity of thiophene was proportional to the amount of CoMoS phases for CVD-Co/MoS_2/Al_2O_3, CVD-Co/MoS_2/TiO_2 and CVD-Co/MoS_2/Al_2O_3. It is concluded that the support does not affect the reactivity of the CoMoS phases in HDS when the catalysts are supported on TiO_2, ZrO_2 and Al_2O_3. In contrast, CoMoS phases on SiO_2 show catalytic features characteristic of CoMoS Type II. On the other hand, the Co species on MoS_2/TiO_2, ZrO_2 and SiO_2 had the same HYD activity for the HYD of butadiene, while the Co species on MoS_2/Al_2O_3 had a higher activity.

It is proposed that the preparation of the model catalysts, as described here, provides valuable insight into the nature of Co–Mo sulfide catalysts: the catalyst structure, the coverage of Co on the edge sites of MoS_2 particles [34], the effects of catalyst preparation [34], the effects of the support [35] and NO adsorption behavior [61].

Acknowledgements

This work has been entrusted by the New Energy and Industrial Technology Development Organization under a subsidy of the Ministry of Economy, Trade and Industry. We are grateful to Dr. T. Fujikawa and Mr. T. Ebihara (Cosmo Research Institute) for carrying out the TEM of the catalysts.

References

[1] H. Topsøe, B.S. Clausen, F.E. Massoth, in: J.R. Anderson, M. Boudart (Eds.), Catalysis—Science and Technology, vol. 11, Springer, Berlin, 1996.
[2] K. Kabe, A. Ishihara, W. Qian, Hydrodesulfurization and Hydrodenitrogenation, Kodansha, Tokyo, 1999.
[3] H. Topsøe, B.S. Clausen, Catal. Rev.-Sci. Eng. 26 (1984) 395.
[4] H. Topsøe, B.S. Clausen, N. Topsøe, E. Pederson, Ind. Eng. Chem. Fund. 25 (1986) 25.
[5] R.R. Chianelli, Catal. Rev. -Sci. Eng. 26 (1984) 361.
[6] R. Prins, V.H.J. de Beer, G.A. Somorjai, Catal. Rev. -Sci. Eng. 31 (1989) 1.
[7] R.R. Chianelli, M. Daage, M.J. Ledoux, Adv. Catal. 40 (1994) 177.
[8] A.N. Startsev, Catal. Rev. -Sci. Eng. 37 (1995) 353.
[9] D.D. Whitehurst, T. Isoda, I. Mochida, Adv. Catal. 42 (1998) 345.
[10] M. Breysse, J.L. Portefaix, M. Vrinat, Catal. Today 10 (1991) 489.
[11] B.S. Clausen, S. Mørup, H. Topsøe, R. Candia, J. Phys. Colloq. 37 (1976) C6-249.
[12] H. Topsøe, B.S. Clausen, R. Candia, C. Wivel, S. Mørup, J. Catal. 68 (1981) 433.
[13] C. Wivel, R. Candia, B.S. Clausen, S. Mørup, H. Topsøe, J. Catal. 68 (1982) 453.
[14] H. Topsøe, B.S. Clausen, R. Candia, C. Wivel, S. Mørup, Bull. Soc. Chim. Belg. 90 (1981) 1189.

[15] R. Candia, O. Sørensen, J. Villadsen, N. Topsøe, B.S. Clausen, H. Topsøe, Bull. Soc. Chim. Belg. 93 (1984) 763.
[16] H. Topsøe, B.S. Clausen, N. Topsøe, P. Zeuthen, Stud. Surf. Sci. Catal. 53 (1989) 77.
[17] S.M.A.M. Bouwens, F.B.M. van Zon, M.P. van Dijk, A.M. van der Kraan, V.H.J. de Beer, J.A.R. van Veen, D.C. Koningsberger, J. Catal. 146 (1994) 375.
[18] M. Breysse, P. Afanasiev, C. Geantet, M. Vrinat, Catal. Today, this volume.
[19] M. Sun, D. Nicosia, R. Prins, Catal. Today, this volume.
[20] F. Luck, Bull. Soc. Chim. Belg. 100 (1991) 781.
[21] J.A.R. van Veen, E. Gerkema, A.M. van der Kraan, A. Knoester, J. Chem. Soc., Chem. Commun. 1684 (1987).
[22] J.A.R. van Veen, E. Gerkema, A.M. van der Kraan, P.A.J.M. Hendriks, H. Beens, J. Catal. 133 (1992) 112.
[23] S.P.A. Louwers, R. Prins, J. Catal. 133 (1992) 94.
[24] L. Medici, R. Prins, J. Catal. 163 (1996) 94.
[25] J.A.R. van Veen, H.A. Colijn, R.A.J.M. Hendriks, J.A. van Welsenes, Fuel Process. Technol. 35 (1993) 137.
[26] F. Maugé, A. Vallet, J. Bachelier, J.C. Duchet, J.C. Lavalley, Catal. Lett. 2 (1989) 57.
[27] F. Maugé, A. Vallet, J. Bachelier, J.C. Duchet, J.C. Lavalley, J. Catal. 162 (1996) 88.
[28] M. Angulo, F. Maugé, J.C. Duchet, J.C. Lavalley, Bull. Soc. Chim. Belg. 96 (1987) 925.
[29] T.R. Halbert, T. Ho, E.I. Stiefel, R.R. Chianelli, M. Daage, J. Catal. 130 (1991) 116.
[30] Y. Okamoto, M. Odawara, H. Onimatsu, T. Imanaka, Ind. Eng. Chem. Res. 34 (1995) 3707.
[31] Y. Okamoto, H. Katsuyama, AIChE J. 43 (1997) 2809.
[32] Y. Okamoto, H. Okamoto, T. Kubota, H. Kobayashi, O. Terasaki, J. Phys. Chem. B 103 (1999) 7160.
[33] Y. Okamoto, T. Kubota, Catal. Surv. Jpn. 5 (2001) 3.
[34] Y. Okamoto, S. Ishihara, M. Kawano, M. Sato, T. Kubota, J. Catal. 217 (2003) 12.
[35] Y. Okamoto, K. Ochiai, M. Kawano, K. Kobayashi, T. Kubota, Appl. Catal. A 226 (2002) 115.
[36] P.L.J. Gunter, J.W. Niemantsverdriet, F.H. Ribeiro, G.A. Somorjai, Catal. Rev.-Sci. Eng. 39 (1997) 77.
[37] A.M. de Jong, H.J. Borg, L.J. van IJzendoorn, V.G.M. Soudant, V.H.J. de Beer, J.A.R. van Veen, J.W. Niemantsverdriet, J. Phys. Chem. 97 (1993) 6477.
[38] G. Kishan, L. Coulier, J.A.R. van Veen, J.W. Niemantsverdriet, J. Catal. 196 (2000) 180.
[39] G. Kishan, L. Coulier, J.A.R. van Veen, J.W. Niemantsverdriet, J. Catal. 200 (2001) 194.
[40] L. Coulier, G. Kishan, J.A.R. van Veen, J.W. Niemantsverdriet, J. Phys. Chem. 106 (2002) 5897.
[41] Y. Sakashita, T. Yoneda, J. Catal. 185 (1999) 487.
[42] S. Helveg, J.V. Lauritsen, E. Laegsgaad, I. Stensgaad, J.K. Nørskov, B.S. Clausen, H. Topsøe, F. Besenbacher, Phys. Rev. Lett. 84 (2000) 951.
[43] L.S. Byskov, J.K. Nørskov, B.S. Clausen, H. Topsøe, J. Catal. 187 (1999) 109.
[44] J.V. Lauritsusen, S.H. Helveg, E. Laegsgaad, I. Stensgaad, B.S. Clausen, H. Topsøe, F. Besenbacher, J. Catal. 197 (2001) 1.
[45] J.V. Lauritsusen, M. Nyberg, R.T. Vang, M.V. Bollinger, B.S. Clausen, H. Topsøe, K.W. Jacobsen, E. Laegsgaad, J.K. Nørskov, F. Besenbacher, Nanotechnology 4 (2003) 385.
[46] Y. Okamoto, A. Maezawa, T. Imanaka, J. Catal. 120 (1989) 29.
[47] A. Maezawa, M. Kitamura, Y. Okamoto, T. Imanaka, Bull. Chem. Soc. Jpn. 61 (1988) 2295.
[48] F.E. Massoth, Adv. Catal. 27 (1978) 265.
[49] W.K. Hall, in: R. Vanselow, R. Howe (Eds.), Chemistry and Physics of Solid Surfaces, vol. IV, Springer, Berlin, 1986, p. 73.
[50] W.K. Hall, in: H.F. Barry, P.C.H. Mitchell (Eds.), Proceedings of the Climax Fourth International Congress on the Chemistry and Uses of Molybdenum, Climax Molybdenum Comp., Ann Arbor, 1982, p. 224.
[51] Y. Okamoto, T. Imanaka, J. Phys. Chem. 92 (1988) 7102.
[52] I. Alstrup, I. Chorkendorff, R. Candia, B.S. Clausen, H. Topsøe, J. Catal. 77 (1982) 397.
[53] N.Y. Topsøe, H. Topsøe, J. Catal. 77 (1982) 293.
[54] Y. Okamoto, Y. Katoh, Y. Mori, T. Imanaka, S. Teranishi, J. Catal. 70 (1981) 445.
[55] K.Y.S. Ng, E. Gulari, J. Catal. 95 (1985) 33.
[56] S. Yoshinaka, K. Segawa, Catal. Today 45 (1998) 293.
[57] D.H. Wang, W. Qian, A. Ishihara, T. Kabe, J. Catal. 203 (2001) 322.
[58] T. Kubota, N. Hosomi, Y. Hamasaki, Y. Okamoto, Proceedings of the Fourth Tokyo Conference on Advanced Catalytic Science and Technology, Stud. Surf. Sci. Catal. 145 (2003) 331.
[59] T. Kubota, N. Hosomi, Y. Hamasaki, Y. Okamoto, Chem. Phys. Lett. 370 (2003) 813.
[60] M. Daage, R.R. Chianelli, J. Catal. 149 (1994) 414.
[61] Y. Okamoto, M. Kawano, T. Kubota, J. Chem. Soc., Chem. Commun. (2003) 1086.